Electromagnetic form factors of odd-A rotational nuclei

P. Sarriguren, E. Graca, and D. W. L. Sprung
Department of Physics, McMaster University, Hamilton, Ontario, Canada L8S 4M1

E. Moya de Guerra
Instituto de Estructura de la Materia, Consejo Superior de Investigaciones Científicas, Serrano 119, 28006 Madrid, Spain

D. Berdichevsky
Department of Physics and Astronomy, Rutgers University, Piscataway, New Jersey 08854
(Received 3 April 1989)

We present a systematic study of single-particle and collective transverse current multipoles in the ground-state band of odd-A axially symmetric deformed nuclei. We analyze the interplay between single-particle and collective contributions to the total transverse form factors for elastic and inelastic scattering in a number of nuclei (^{169}Tm, ^{177,179}Hf, ^{239}Pu), which exemplify different possibilities of ground-state k^π bands ($\frac{1}{2}^+, \frac{7}{2}^-, \frac{9}{2}^+$) and of odd-$Z$ or odd-N character. We also discuss the dependence of form factors and static moments on the mean field used to generate the ground-state wave function. The dominant contribution is found to come from the odd nucleon, except in the low momentum transfer region ($q < 1$ fm^{-1}) where the core is manifest through its interference with the single-particle amplitude.

I. INTRODUCTION

In a previous paper[1] we presented a detailed analysis of transverse form factors of rotational even-even nuclei. We discussed results of numerical calculations for ^{154}Sm,^{156,158}Gd,^{164}Dy,^{166,168}Er,^{174}Yb based on both the projected Hartree-Fock (PHF) approach and on the cranking model, using HF+BCS wave functions obtained with different effective interactions. We discussed the dependence of the form factors on the mean field used to generate the ground-state wave function, and on various assumptions about the nature of the rotational mode. In this paper we present a similar analysis for rotational odd-A nuclei.

In the odd-A case, the transverse form factors receive two types of contributions:[2,3] collective and single particle. The former come from the even-even core and are similar to those of even-even nuclei; the latter come from the odd particle and depend strongly on the single-particle state occupied by the unpaired nucleon. The analysis made in Ref. 1 applies as well to the collective contributions in odd-A nuclei. Hence, in the present work we place special emphasis on single-particle contributions, on the interplay between the two types of contributions, and their relative intensities in the entire q range $q \leq 2.5$ fm^{-1} of experimental interest.

The single-particle form factors are sensitive to the quantum number k of the band, to the character (neutron or proton) of the odd nucleon, and to the mean field used to generate the single-particle states. In Ref. 4 several rare-earth odd-proton nuclei with $k > \frac{1}{2}$ were studied. In order to cover other possibilities, we analyze here ^{177}Hf and ^{179}Hf as examples of odd-neutron $k > \frac{1}{2}$ nuclei with $k = \frac{7}{2}$ and $k = \frac{9}{2}$, respectively, and ^{169}Tm,^{239}Pu as examples of odd-proton and odd-neutron $k = \frac{1}{2}$ nuclei. Special attention is paid to the $k = \frac{1}{2}$ bands, where the interplay between core and single-particle aspects is much more involved. To analyze the effect of the mean field we use HF+BCS wave functions of the Sk-3 (Ref. 5) and Ska (Ref. 6) effective interactions, as well as Nilsson single-particle states.

The paper is organized as follows. The theory is summarized in Sec. II and details of the calculations are given in Sec. III. Results of numerical calculations are presented and discussed in Secs. IV and V for $k = \frac{1}{2}$ (^{239}Pu,^{169}Tm) and $k > \frac{1}{2}$ (^{177}Hf,^{179}Hf) bands, respectively. Form factors for elastic and inelastic scattering as well as intrinsic form factors and static moments are considered in all cases. The final remarks and conclusions are summarized in Sec. VI.

II. SUMMARY OF THE THEORY

Following the notation of Ref. 2, we can write the transverse electromagnetic form factors of axially symmetric deformed nuclei, in plane-wave Born approximation and for a transition within the ground-state band $I_i k \rightarrow I_f k$, as

$$|F_T(q)|^2_{I_i k \rightarrow I_f k} = \sum_{\lambda=\text{even}>0} [F^{E\lambda}_{I_f}(q)]^2 + \sum_{\lambda=\text{odd}} [F^{M\lambda}_{I_f}(q)]^2 , \quad (1)$$

where the electric (E) and magnetic (M) multipole form factors can be expressed in terms of intrinsic matrix ele-

ments weighted by angular momentum dependent coefficients. These expressions were developed in the context of an expansion in powers of the total angular momentum operator I_μ. To lowest order in this expansion, the intrinsic multipoles are independent of the particular transition considered and depend only on the intrinsic structure of the ground-state band.[3] Denoting by $\mathcal{F}^{\sigma\lambda}$ ($\sigma=E,M$) the q-dependent intrinsic multipoles, the transition multipoles for the case $I_f \geq I_i = k$, can be written as

$$F^{E\lambda}_{I_f} = [I_f(I_f+1) - I_i(I_i+1)]\langle I_i k \lambda 0 | I_f k\rangle \mathcal{F}^{E\lambda}_R + (-1)^{I_i-k}\langle I_i -k \lambda 2k | I_f k\rangle \mathcal{F}^{E\lambda}_{2k} , \tag{2a}$$

$$F^{M\lambda}_{I_f} = \langle I_i k \lambda 0 | I_f k\rangle \mathcal{F}^{M\lambda}_k + (-1)^{I_i-k}\langle I_i -k \lambda 2k | I_f k\rangle \mathcal{F}^{M\lambda}_{2k} + \frac{k(k+1)+\lambda(\lambda+1)-I_f(I_f+1)}{\sqrt{2\lambda(\lambda+1)}} \times \langle k k \lambda 0 | I_f k\rangle \mathcal{F}^{M\lambda}_R . \tag{2b}$$

Here, $\mathcal{F}^{\sigma\lambda}_R$ are the transverse multipoles of the collective rotational current (rotational multipoles) that depend on the nuclear rotational model used to describe the band. Their explicit expressions can be found in Ref. 2.

The single-particle intrinsic multipoles $\mathcal{F}^{M\lambda}_k, \mathcal{F}^{\sigma\lambda}_{2k}$ depend only on the single-particle intrinsic wave function of the odd nucleon if the even-even core is time-reversal invariant as we assume in this work. They are different from zero only for $k\neq 0$ bands and are given by[2]

$$\mathcal{F}^{M\lambda}_k = \frac{\sqrt{4\pi}}{Z}\langle \chi_k | \hat{T}^{M\lambda}_0 | \chi_k\rangle , \tag{3a}$$

$$\mathcal{F}^{M\lambda}_{2k} = \frac{\sqrt{4\pi}}{Z}\langle \chi_k | \hat{T}^{M\lambda}_{2k} | \chi_{\bar{k}}\rangle + \delta_{k,1/2}\frac{a}{\sqrt{2}}\mathcal{F}^{M\lambda}_R , \tag{3b}$$

$$\mathcal{F}^{E\lambda}_{2k} = \frac{\sqrt{4\pi}}{Z}\langle \chi_k | \hat{T}^{E\lambda}_{2k} | \chi_{\bar{k}}\rangle - \delta_{k,1/2} a\sqrt{\lambda(\lambda+1)}\mathcal{F}^{E\lambda}_R \tag{3c}$$

where a factor $\sqrt{4\pi}/Z$ has been included in all the definitions of the intrinsic form factors for consistency with our earlier paper. $\hat{T}^{\sigma\lambda}_m$ is the m component of the $\sigma\lambda$ tensor operator,[7] χ_k and $\chi_{\bar{k}}$ are the wave functions of the odd nucleon and its time reverse, respectively, and $a = \langle \chi_k | j_+ | \chi_{\bar{k}}\rangle$ is the decoupling parameter.

Finally, it is also useful to write the long wavelength limit of the intrinsic form factors in order to relate them to the static moments, as well as to check the internal consistency of the calculations. These limits for the $M1$ intrinsic multipoles are given by

$$\lim_{q\to 0}\mathcal{F}^{M1}_R = \frac{-q}{\sqrt{6}ZM} g_R \tag{4a}$$

$$\lim_{q\to 0}\mathcal{F}^{M1}_k = \frac{-q}{\sqrt{6}ZM} k g_k \tag{4b}$$

$$\lim_{q\to 0}\mathcal{F}^{M1}_{2k} = \frac{-q}{\sqrt{6}ZM}\frac{1}{\sqrt{2}}(g_k - g_R)b, \quad (k=\tfrac{1}{2}\text{ only}) . \tag{4c}$$

It is useful for later reference to write explicit expressions for g_k and b as well as for the rotational energy and magnetic moments:

$$k g_k = \langle \chi_k | \hat{\mu}_0 | \chi_k\rangle , \tag{5}$$

$$(g_k - g_R)b = a g_R - \langle \chi_k | \hat{\mu}_+ | \chi_{\bar{k}}\rangle = \sqrt{2} g_{2k} , \tag{6}$$

$$E^I_{\rm rot} = \frac{1}{2\mathcal{J}}[I(I+1) - k^2 + \delta_{k,1/2}(-1)^{I+1/2}(I+1/2)a] , \tag{7}$$

$$\mu = g_R I + \frac{k^2}{I+1}[g_k - g_R + \delta_{k,1/2}(-1)^{I+1/2} \times (2I+1)\sqrt{2} g_{2k}] , \tag{8}$$

where the operator $\hat{\mu}$ is

$$\hat{\mu} = \sum_i (g^i_l l_i + g^i_s s_i)$$

and $\mathcal{J}$ is the moment of inertia, whose value will depend on the particular model employed.

It is clear that the calculated form factors will depend on the rotational model used to describe the band, and on the interaction used to determine the mean field. If a sufficiently extended basis of states is employed to express the wave functions, results should be independent of the basis. In Ref. 1 we discussed all of these aspects as they apply to the rotational multipoles. Here, we complete this analysis by studying the effect of the mean field on the single-particle wave functions. We use for that purpose HF+BCS wave functions of the Sk-3 and Ska effective interactions, as well as Nilsson single-particle states.

III. DETAILS OF THE CALCULATIONS

As mentioned earlier, in Ref. 1 we analyzed the predictions of different rotational models for the collective transverse form factors in even-even nuclei (projected Hartree-Fock and cranking as microscopic models; rigid rotor and irrotational flow as macroscopic models), comparing their predictions for different multipolarities and nuclei. We also studied the dependence of these form factors on the mean field and on the basis truncation parameter. As a result, in this work we take the value $E_{\rm cut}=30$ MeV for the cutoff parameter of the basis states, because it provides good convergence for the form factors. In addition, the analysis of the model dependence carried out there showed important differences among the predictions of the rotational models for some multipolarities (i.e., $E2$). Comparison with the experimental data available at low momentum transfer (see Table V of Ref. 1) gave us confidence in the cranking model as a description of the rotational band. Since we already know what kind of behavior is expected for the different rotational models considered, and since in this paper we are mainly interested in the single-particle contributions and in their relative importance as compared to the collective ones, results for the collective form factors will be shown here for the cranking model only. Finally, the same kind of arguments for using the Sk-3 and Ska

TABLE I. Input parameters for the Hartree-Fock ($b_0, q_0, \Delta_p, \Delta_n$) and Nilsson ($\kappa, \mu, \beta, b_{osc}$) calculations (see text).

	b_0 (fm^{-1})	q_0	Δ_p (MeV)	Δ_n (MeV)	b_{osc} (fm)	κ	μ	β
^{169}Tm	0.492	1.200	0.910	0.766	2.35	0.0637	0.600	0.318
^{239}Pu	0.485	1.275	0.740	0.590	2.50	0.0450	0.550	0.270
^{177}Hf	0.490	1.200	0.884	0.698	2.34	0.0637	0.420	0.275
^{179}Hf	0.490	1.200	0.884	0.698	2.37	0.0637	0.420	0.285

effective interactions to generate the mean field apply here, in this case to study how sensitive the single-particle wave functions are to the interaction.

For odd-A nuclei, the fields corresponding to the different interactions were obtained by doing one iteration from the corresponding self-consistent field of the closest even-even nucleus, selecting the orbital occupied by the odd nucleon according to the experimental k and parity. We blocked this state from the BCS calculation, and assigned a pair occupation probability of 0.5. Ten major shells of the axially symmetric oscillator well in cylindrical coordinates were used to define the basis states in the Hartree-Fock case.[8] The Nilsson model states were also used to compute the single-particle form factors.

The effect of doing several more iterations from the even-even case, in order to see how the extra particle polarizes the core, was studied in Ref. 9 without observing significant changes. We repeated these calculations looking for some effect on the form factors, but again the changes were negligible. All of the results presented are then for one iteration.

We also point out that all the intrinsic form factors shown in this paper contain the same center of mass and finite nucleon size corrections as used in Ref. 1. Namely, the dipole expression was used for the nucleon magnetic form factors. For the proton electric form factors we used the sum of monopoles fitted in Ref. 10 and for the electric neutron form factors a difference of two Gaussians[11] was used.

Before entering into our discussion of the results, we present in Table I the input values for the HF+BCS and Nilsson calculations for the nuclei considered. In this table, b_0, q_0, and $\Delta_{n,p}$ are HF parameters while κ, μ, β, and b_{osc} pertain to the Nilsson calculations. In particular, b_0 is the inverse of the oscillator length, q_0 is the axis ratio ($\omega_\perp/\omega_z$) used in the deformed Hartree-Fock basis,[8] and $\Delta_{p,n}$ stand for the gap parameters for protons and neutrons determined from experimental mass differences. κ and μ are the Nilsson potential parameters taken from Refs. 12 and 13. However, for ^{239}Pu better results for g_k and μ_I were obtained by slightly altering the standard values to those given in Table I. The adopted values follow the general trend of reducing κ in heavier nuclei.[14] The deformation β is fixed according to the experimental value of the quadrupole moment[15] and is in good agreement with the Hartree-Fock results. The oscillator length is taken as $b_{osc} = A^{1/6}$ fm. The difference between the oscillator length b_0^{-1} in the self-consistent calculation and b_{osc} used in the Nilsson calculation is consistent with the dependence of b_0 on the basis size, as studied in Ref. 16. In Table II the results for binding energies, radii, and quadrupole moments obtained with Sk-3 and Ska are shown.

IV. $k = \frac{1}{2}$ BANDS: ^{239}Pu AND ^{169}Tm

In this section we discuss ^{169}Tm and ^{239}Pu, examples of $k = \frac{1}{2}$ rotational nuclei with an odd-proton and odd-neutron, respectively. First of all we summarize the experimental data available at present from which one can infer experimental values for the form factors at very low momentum transfer [see Eq. (4)], and compare them with the theoretical predictions. One can also use these expressions to check the internal consistency of the calculations by comparing the results obtained for the intrinsic form factors at low q with the values of g_k, $(g_k - g_R)b$, a, and g_R obtained from their definitions in Eqs. (5) and (6). For momentum transfers $q < 0.1$ fm^{-1} we found agreement in all the cases within 0.3%, which gives us confidence in the calculations.

From the experimental energy spectra for these nuclei[17,18] the moment of inertia ($\mathcal{I}$) and the decoupling parameter can be extracted by using the expressions for the

TABLE II. Results obtained for binding energies, charge radii, proton and neutron radii, and quadrupole moments with the Sk-3 and Ska effective interactions.

			$\langle r^2 \rangle^{1/2}$ (fm)			Q_2 (fm^2)	
		B (MeV)	c	p	n	p	n
^{169}Tm	Sk-3	1359.76	5.352	5.296	5.380	804.13	1146.7
	Ska	1358.92	5.307	5.250	5.405	824.55	1173.7
^{239}Pu	Sk-3	1787.71	5.949	5.898	5.989	1116.4	1709.9
	Ska	1787.96	5.891	5.838	6.013	1170.6	1816.3
^{177}Hf	Sk-3	1413.16	5.422	5.366	5.454	721.44	1064.1
	Ska	1412.89	5.375	5.318	5.479	743.91	1106.4
^{179}Hf	Sk-3	1427.26	5.422	5.366	5.464	721.44	1068.9
	Ska	1427.00	5.375	5.318	5.493	743.91	1112.1

TABLE III. Results obtained for $\langle J_\perp^2 \rangle$, $\mathcal{I}_{\text{cranking}}$, and g_R (in PHF and cranking models) for Sk-3 and Ska forces. Experimental values for $\mathcal{I}$ and g_R are also shown.

		$\langle J_\perp^2 \rangle_p$	$\langle J_\perp^2 \rangle_n$	$\langle J_\perp^2 \rangle_{\text{total}}$	$\mathcal{I}_p$	$\mathcal{I}_n$	$\mathcal{I}_{\text{total}}$	g_R PHF	g_R cranking
^{169}Tm	exp						40.36		0.41
	Sk-3	58.55	89.41	148.0	10.70	20.16	30.86	0.391	0.341
	Ska	62.28	92.98	155.3	10.70	21.37	32.08	0.395	0.304
^{239}Pu	exp						79.98		0.39
	Sk-3	78.75	134.2	213.0	20.68	39.27	59.55	0.363	0.325
	Ska	91.01	143.0	234.0	21.61	36.97	58.59	0.384	0.367
^{177}Hf	exp						39.84		0.265
	Sk-3	48.18	82.04	130.2	8.854	20.28	29.13	0.362	0.283
	Ska	51.41	85.32	136.7	8.817	20.36	29.18	0.365	0.268
^{179}Hf	exp						44.82		0.156
	Sk-3	48.18	89.34	137.5	8.854	25.40	34.25	0.323	0.189
	Ska	51.41	90.02	141.4	8.817	23.60	32.42	0.340	0.205

rotational energy [Eq. (7)]. The experimental values quoted for a and $\mathcal{I}$ in Tables III and IV were obtained using the two first excited states of the band. With these values good agreement for the remaining excitation energies was found up to spin of $\frac{13}{2}$, demonstrating the validity of the rotational model for these particular nuclei.

We also have experimental magnetic dipole moments[18] up to $I=\frac{7}{2}$ for ^{169}Tm but only for $I=\frac{1}{2}$ in ^{239}Pu. The values of μ ($I=\frac{1}{2},\frac{3}{2},\frac{5}{2}$) of ^{169}Tm allow us to obtain experimental values for g_k, g_R, and b according to the general expression for the magnetic moment given in Eq. (8). This analysis leads to the following combinations:

$$g_R=-\tfrac{1}{4}\mu_{1/2}+\tfrac{1}{6}\mu_{3/2}+\tfrac{7}{20}\mu_{5/2}\ ,$$

$$g_k=g_R+\tfrac{23}{4}\mu_{1/2}+\tfrac{13}{6}\mu_{3/2}-\tfrac{49}{20}\mu_{5/2}\ ,$$

$$(g_k-g_R)b=-\tfrac{1}{2}\mu_{1/2}+\tfrac{4}{3}\mu_{3/2}-\tfrac{7}{10}\mu_{5/2}\ ,$$

from which the experimental values of g_k, g_R, and b (magnetic decoupling parameter) quoted in Table IV for ^{169}Tm were obtained. These results are in excellent agreement with experimental values

$$g_k=-1.57,\quad g_R=0.406,\quad b=-0.16$$

in Ref. 19 and

$$g_k=-1.65(\pm 0.06),\quad g_R=0.419(\pm 0.01)$$

in Ref. 20. For ^{239}Pu we took the experimental values of Ref. 21 based on $(\alpha,3n)$ reactions.

Table III contains the moments of inertia and gyromagnetic ratios computed with the Sk-3 and Ska interactions. For completeness, the values of $\langle J_\perp^2 \rangle$ and $g_{R,\text{PHF}}$ are included. We observe that the values obtained for the moments of inertia are systematically smaller than experiment. This can be related[8] to the fact that for HF calculations with Skyrme-type forces, the single-particle energies are too spread out near the Fermi surface (effective mass less than unity).

TABLE IV. Values of a, g_k, $(g_k-g_R)b$, and μ_I for different spins obtained with the HF (Sk-3 and Ska) and the Nilsson model for the $k=\frac{1}{2}$ nuclei ^{169}Tm and ^{239}Pu. Also shown are the experimental values and (in brackets) the magnetic moments evaluated with effective g_s factors.

		a	g_k	$(g_k-g_R)b$	$\mu_{1/2}$	$\mu_{3/2}$	$\mu_{5/2}$	$\mu_{7/2}$	$g_{s_{\text{eff}}}/g_{s_{\text{free}}}$
^{169}Tm	exp	−0.77	−1.67	0.27	−0.232	0.515	0.761	1.341	
	Sk-3	−0.66	−3.06	0.18	−0.455	0.241	0.533	1.081	
					(−0.253)	(0.416)	(0.594)	(1.198)	(0.719)
	Ska	−0.62	−3.13	0.21	−0.490	0.197	0.425	0.967	
					(−0.273)	(0.374)	(0.496)	(1.083)	(0.710)
	Nilsson	−0.88	−2.37	−0.08	−0.231	0.302	0.858	1.238	
					(−0.157)	(0.421)	(0.853)	(1.332)	(0.830)
^{239}Pu	exp	−0.58	1.28	0.43	0.203				
	Sk-3	−0.93	2.04	0.59	0.253	0.894	0.685	1.494	
					(0.237)				(0.626)
	Ska	−0.90	2.28	0.44	0.355	0.918	0.863	1.586	
					(0.301)				(0.561)
	Nilsson	−1.29	1.44	0.68	0.144	0.966	0.766	1.736	
					(0.161)				(0.888)

In Table IV one finds g_k, the decoupling (a) and magnetic decoupling (b) parameters and the magnetic moments evaluated from them, for the Nilsson model and for the Sk-3, Ska effective interactions. Equations (5) and (6) were used for the HF calculations. For the Nilsson model, more explicit expressions[2] can be found in terms of the basis coefficients:

$$(\hat{j}\equiv\sqrt{2j+1})$$

$$g_k=g_l^k+\frac{\mu_s^k-\frac{1}{2}g_l^k}{k}\sum_{Nj,j'}C_{Nlj}^kC_{Nl'j'}^k(-1)^{N+j-1/2}\times\sqrt{6}W(\tfrac{1}{2}\tfrac{1}{2}jj';1l)\langle jk10|j'k\rangle\hat{j} \tag{9}$$

$$(g_k-g_R)b=(g_R-g_l^k)a+(g_s^k-g_l^k)\sum_{Nj,j'}C_{Nlj}^kC_{Nl'j'}^k\times(-1)^N\sqrt{3}W(\tfrac{1}{2}\tfrac{1}{2}jj';1l)\times\langle j-\tfrac{1}{2}11|j'\tfrac{1}{2}\rangle\hat{j} \tag{10}$$

$$a=\sum_{Nj}(C_{Nlj}^k)^2(-1)^{j-1/2}(j+\tfrac{1}{2})\ . \tag{11}$$

These coefficients C_{Nlj}^k determine the expansion of the single-particle state in the spherical n,l,j basis

$$|k\rangle=\sum_{Nj}C_{Nlj}^k|Nlj\Omega_k\rangle\ . \tag{12}$$

For the parameters κ,μ of Table I, and for the single-particle states $\frac{1}{2}^+[411]$ for ^{169}Tm and $\frac{1}{2}^+[631]$ for ^{239}Pu in the asymptotic quantum number notation, these coefficients take the following values:

^{169}Tm $C_{0,1/2}=0.3059$, $C_{2,3/2}=0.7253$,
$C_{2,5/2}=0.4525$, $C_{4,7/2}=0.3970$,
$C_{4,9/2}=0.1346$;

^{239}Pu $C_{0,1/2}=-0.3083$, $C_{2,3/2}=-0.5631$,
$C_{2,5/2}=0.0845$, $C_{4,7/2}=0.3963$,
$C_{4,9/2}=0.4294$, $C_{6,11/2}=0.4595$,
$C_{6,13/2}=0.1679$.

By the use of reasonable effective g_s factors in order to take into account important effects not included in present HF calculations such as first-order spin polarization of the core by the odd nucleon,[22] the agreement with the experimental magnetic moments is improved in most cases. In the bracketed entries of Table IV, one can see these new values for μ_I evaluated with $g_{s_{\text{eff}}}$. The $g_{s_{\text{eff}}}$ were determined by fitting the experimental g_k to the expression

$$g_k=g_l+(g_s-g_l)\frac{\langle k|s_z|k\rangle}{k} \tag{13}$$

easily obtained from the definition in Eq. (5). We find $g_{s_{\text{eff}}}/g_{s_{\text{free}}}\sim 0.7$ in agreement with a similar analysis by Bohr and Mottelson.[23]

The use of $g_{s_{\text{eff}}}$ primarily affects the magnetic moments of the $I=\frac{1}{2},\frac{3}{2}$ states. For higher spin states the magnetic moment is mainly determined by the g_RI term, and reasonable agreement is found in most cases. Since the intrinsic form factors at low q are proportional to the static parameters, in the region $q<0.1$ fm^{-1}, the form factors compare to experiment in a similar manner as the corresponding parameters do.

A. Intrinsic form factors

Figure 1 gives the results for the single-particle intrinsic form factors for ^{169}Tm (a) and ^{239}Pu (b). The multipolarities shown ($M1$,$M3$ and $E2$,$E4$) cover elastic scattering $\frac{1}{2}\rightarrow\frac{1}{2}$ and inelastic processes up to the $\frac{1}{2}\rightarrow\frac{7}{2}$ transitions. This figure shows the magnetic intrinsic multipoles $\mathcal{F}_k^{M1,3}$ and the pure single-particle contribution to $\mathcal{F}_{2k}^{\sigma\lambda}$ denoted $\mathcal{F}_{2k}^{\sigma\lambda}$(s.p.). According to Eq. (3),

$$\mathcal{F}_{2k}^{\sigma\lambda}(\text{s.p.})=\frac{\sqrt{4\pi}}{Z}\langle\chi_k|\hat{T}_{2k}^{\sigma\lambda}|\chi_{\bar{k}}\rangle\ . \tag{14}$$

The contributions coming from the subscript k and $2k$ pieces have been plotted separately because they enter into the total form factor [Eq. (2)] with different spin-dependent coefficients, and then their combination is no longer "intrinsic." In the particular case of the electric multipoles, we only have $2k$ contributions and then the total single-particle form factor is always proportional to it. The solid, dotted, and dashed lines represent the Sk-3 interaction, the Ska interaction, and the Nilsson model, respectively. The similarity between Sk-3 and Ska predictions is apparent for all multipoles in both nuclei. The Nilsson model shows the same general trend in the peak structure, but with some noticeable differences.

One reason for these differences is the fact that the Nilsson wave functions contain only components of a single major shell, while the HF wave functions have sizable components from other shells. As an example for ^{169}Tm the $N=4$ orbitals represent 63% of the HF wavefunction normalization while $N=2$ accounts for 13% and $N=6$ for 22%, with small contributions from other shells. For ^{239}Pu only 51% is due to $N=6$ components, with 16% from $N=4$ and 29% from $N=8$.

It is also interesting to look at the spin and convection contributions to these intrinsic form factors. We have not drawn these contributions separately but their examination reveals interesting interplay. It is evident for the odd-neutron case (^{239}Pu) that the magnetization of the neutron is always dominant, and then the single-particle contribution comes almost entirely from the magnetic properties of the odd neutron. On the other hand, in the odd-proton case both contributions are comparable and their combination can produce different effects according to their relative sign. The first $\mathcal{F}_k^{M1}$ peak in ^{169}Tm occurs near $q=0.3$ fm^{-1}. Here, magnetization is dominant but convection is also important and opposite in sign, reduc-

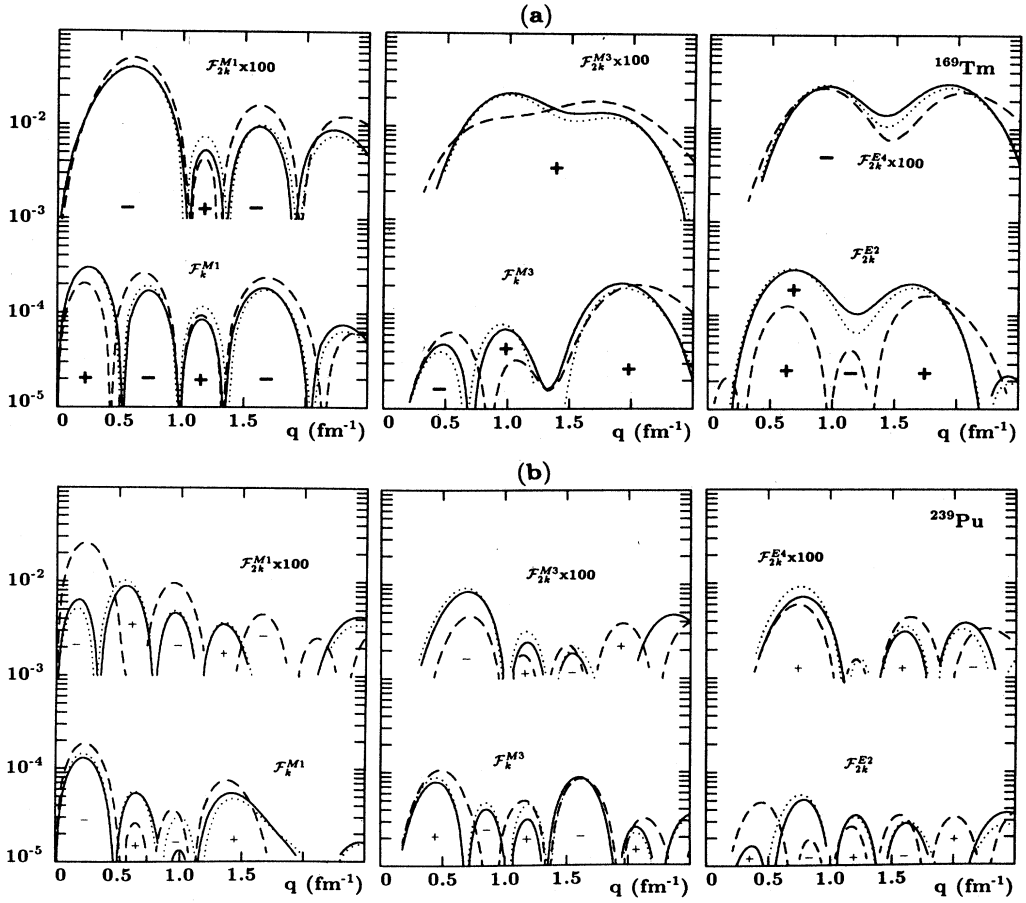

FIG. 1. Intrinsic single-particle $M1,3$ and $E2,4$ form factors of ^{169}Tm (a) and ^{239}Pu (b). Results are for Sk-3 (solid), Ska (dotted), and Nilsson (dashed).

ing the magnitude of this peak by a factor 2. The $\mathcal{F}^{M1}_{2k}$ multipole is dominated by convection at low q ($q<0.3$ fm^{-1}) and by magnetization for $0.3<q<1$ fm^{-1}; in the latter case the contributions add. As a result, a broad and important first peak appears in $\mathcal{F}^{M1}_{2k}$ destroying the double peak structure of the spin contribution. Similar remarks apply to the $\mathcal{F}^{M3}_{k}$ case with a dominant magnetization contribution reduced by 50% by the convection contribution in the first peak up to 0.6 fm^{-1}, and to $\mathcal{F}^{M3}_{2k}$ where there is almost a cancellation for $q<0.2$ fm^{-1} and magnetization dominates after that with corrections adding constructively in a range of q up to 2 fm^{-1}. The electric multipoles $\mathcal{F}^{E2}_{2k}$ and $\mathcal{F}^{E4}_{2k}$ are dominated by the convection part for $q<0.1$ fm^{-1} but magnetization is dominant afterwards. Things are not very different in the Nilsson model.

B. Transition form factors

Form factors are shown in Figs. 2–5 for the corresponding elastic process $\frac{1}{2}\rightarrow\frac{1}{2}$, and transitions $\frac{1}{2}\rightarrow\frac{3}{2}$, $\frac{1}{2}\rightarrow\frac{5}{2}$, and $\frac{1}{2}\rightarrow\frac{7}{2}$. In all of these figures part (a) is for ^{169}Tm and (b) for ^{239}Pu. These figures show the interplay of collective and single-particle contributions and the importance of the contribution proportional to the decoupling parameter, for these $k=\frac{1}{2}$ nuclei. For each multipolarity we show the squared single-particle contributions (dotted lines) for the multipole and transition under consideration

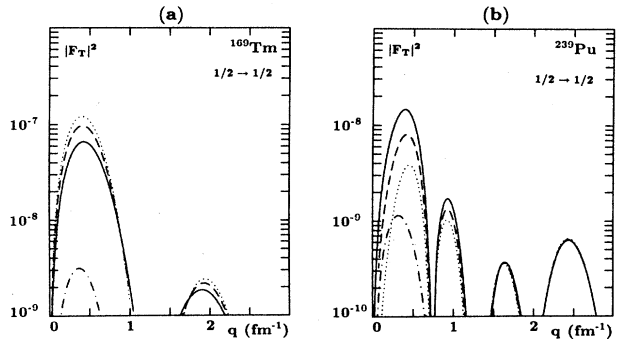

FIG. 2. Total transverse form factor squared (solid) for the elastic case: for ^{169}Tm (a) and ^{239}Pu (b). Also shown are the core contribution (dash-dotted), the single-particle contribution (dotted), and the change in the single particle due to addition of the decoupling parameter term (dashed) (see text).

$$|F^{\sigma\lambda}_{I_f}(\text{s.p.})|^2=[\langle I_i k\lambda 0|I_f k\rangle \mathcal{F}^{\sigma\lambda}_k + \langle I_i -k\lambda 2k|I_f k\rangle \mathcal{F}^{\sigma\lambda}_{2k}(\text{s.p.})]^2 . \quad (15)$$

The dashed lines represent

$$[\langle I_i k\lambda 0|I_f k\rangle \mathcal{F}^{\sigma\lambda}_k + \langle I_i -k\lambda 2k|I_f k\rangle \mathcal{F}^{\sigma\lambda}_{2k}]^2 ,$$

where $\mathcal{F}_{2k}$ now contains the core contribution $a\mathcal{F}_R$ [Eq. (3)]. In these expressions only the subscript-$2k$ term survives for the electric case. The dash-dotted lines are the core contributions proportional to $[\mathcal{F}^{\sigma\lambda}_R]^2$ using the cranking model. The solid line is the total result $|F^{\sigma\lambda}_{I_f}|^2$ given by Eq. (1). Since we have seen the effect of the interaction in the single-particle form factors and we know how the core is affected by them, we present calculations only for the Sk-3 force.

From Fig. 2 one can learn some basic features of the interplay between the various contributions. For transverse elastic scattering $\frac{1}{2}\rightarrow\frac{1}{2}$ only the $M1$ multipole is different from zero and the transition form factor has the following explicit expression:

$$F^2_T=|F^{M1}_{1/2}|^2 = [\langle \tfrac{1}{2}\tfrac{1}{2}10|\tfrac{1}{2}\tfrac{1}{2}\rangle \mathcal{F}^{M1}_k + \langle \tfrac{1}{2}-\tfrac{1}{2}11|\tfrac{1}{2}\tfrac{1}{2}\rangle \mathcal{F}^{M1}_{2k} + \langle \tfrac{1}{2}\tfrac{1}{2}10|\tfrac{1}{2}\tfrac{1}{2}\rangle \mathcal{F}^{M1}_R]^2 .$$

The dotted line is simply

$$\tfrac{1}{3}[\mathcal{F}^{M1}_k - \sqrt{2}\mathcal{F}^{M1}_{2k}(\text{s.p.})]^2 ,$$

and from Fig. 1 one can understand its behavior. In the range $q<1$ fm^{-1} where the main peak occurs, one sees that for ^{169}Tm there is a destructive combination between k and $2k$ for $0.5<q<1$ fm^{-1}, but the important $2k$ contribution is clearly dominant. On the other hand, for ^{239}Pu, k and $2k$ combine destructively in the whole range considered and as a result the total single-particle (dotted) contribution is one order of magnitude smaller than the equivalent for ^{169}Tm. This is interesting because the

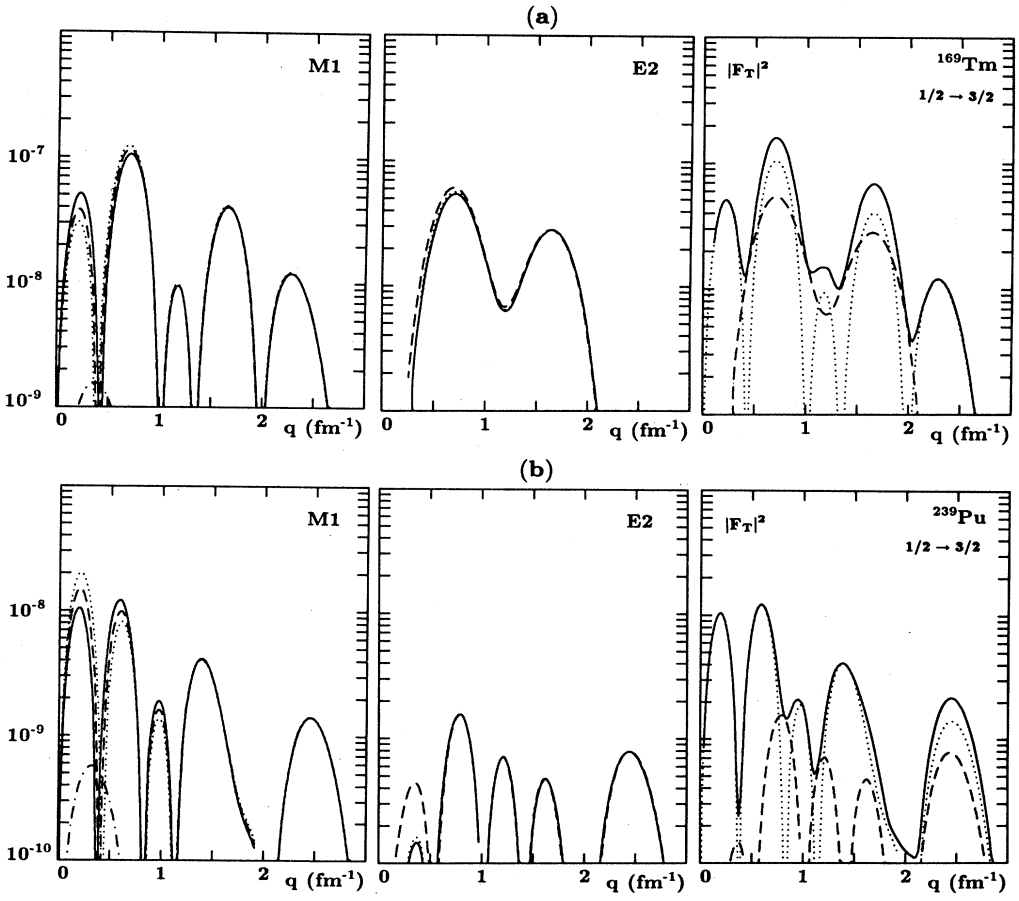

FIG. 3. Total transverse form factor squared for the transition $\frac{1}{2}\rightarrow\frac{3}{2}$ in ^{169}Tm (a) and ^{239}Pu (b). Each multipolarity ($M1$ and $E2$) is divided into the same contributions as in Fig. 2. The total form factor in the rightmost panels (solid) is the sum of $M1$ (dotted) and $E2$ (dashed) multipoles.

core contributions are comparable and very important collective effects now appear in the total form factor. The dashed lines correspond to the addition of the term proportional to the decoupling parameter in the $2k$ part. As seen in Fig. 2, this produces a reduction in the peak for ^{169}Tm and an enhancement for ^{239}Pu. The reason for this is that in both cases the decoupling parameter and the first peak of the $M1$ core contribution are negative, while the single-particle contributions have opposite signs. Finally, the core contribution is added to produce the total form factor. The net effect of the core is to reduce the pure single-particle contribution of ^{169}Tm by a factor 2 and to increase it in ^{239}Pu by a factor 4.

It is also worth mentioning that in the range of q between 0 and 1 fm^{-1} the $k=\frac{1}{2}$ odd-neutron nuclei are more sensitive to the $a\mathcal{F}_R^{\sigma\lambda}$ term. In this case the convection part of $\mathcal{F}_{2k}$ that was almost zero receives a contribution from the core that (due to a cancellation between proton and neutron magnetizations[1]) is almost entirely a proton convection contribution. For this case, the proportionality between the form factors and the static parameters at low momentum transfer extends to larger q. One can see, for instance, how the relation between the first peaks of the $M1$ multipole in ^{169}Tm and ^{239}Pu is the same as the relation between their theoretical magnetic moments $\mu_{1/2}$, once the square in the form factor has been removed.

In Fig. 3 the transition $\frac{1}{2}\rightarrow\frac{3}{2}$ is analyzed by the decomposition of each multipole ($M1$,$E2$) into the same kind of contributions as in Fig. 2. The last frame of the figure shows the total form factor [Eq. (1)]. It is worthwhile to compare how the same multipole ($M1$ in this case) acquires very different shapes for different transitions. In both nuclei there is a single first peak in $I_f=\frac{1}{2}$ which splits into two peaks for $I_f=\frac{3}{2}$. This is the result of different spin-dependent coefficients. Because $\langle\frac{1}{2}\frac{1}{2}10|\frac{3}{2}\frac{1}{2}\rangle=\sqrt{2/3}$ and $\langle\frac{1}{2}-\frac{1}{2}11|\frac{3}{2}\frac{1}{2}\rangle=\sqrt{1/3}$, the combination between $\mathcal{F}_k$ and $\mathcal{F}_{2k}$ is the opposite to what we had earlier. The core effect is not so important in ^{239}Pu in this case because the single-particle contributions add constructively and then the core contribution is much smaller in comparison.

The $E2$ multipole is very easily understood by looking at the intrinsic single-particle multipole of Fig. 1. Since now $\mathcal{F}_{2k}^{E\lambda}$ is the only single-particle contribution, the dotted line is simply the square of this intrinsic multipole with a spin-dependent coefficient. The effect of the decoupling parameter in the first peak is the same in both cases because we have a positive pure single-particle (Fig. 1) form factor with a negative coefficient ($-\sqrt{3}/5$), and

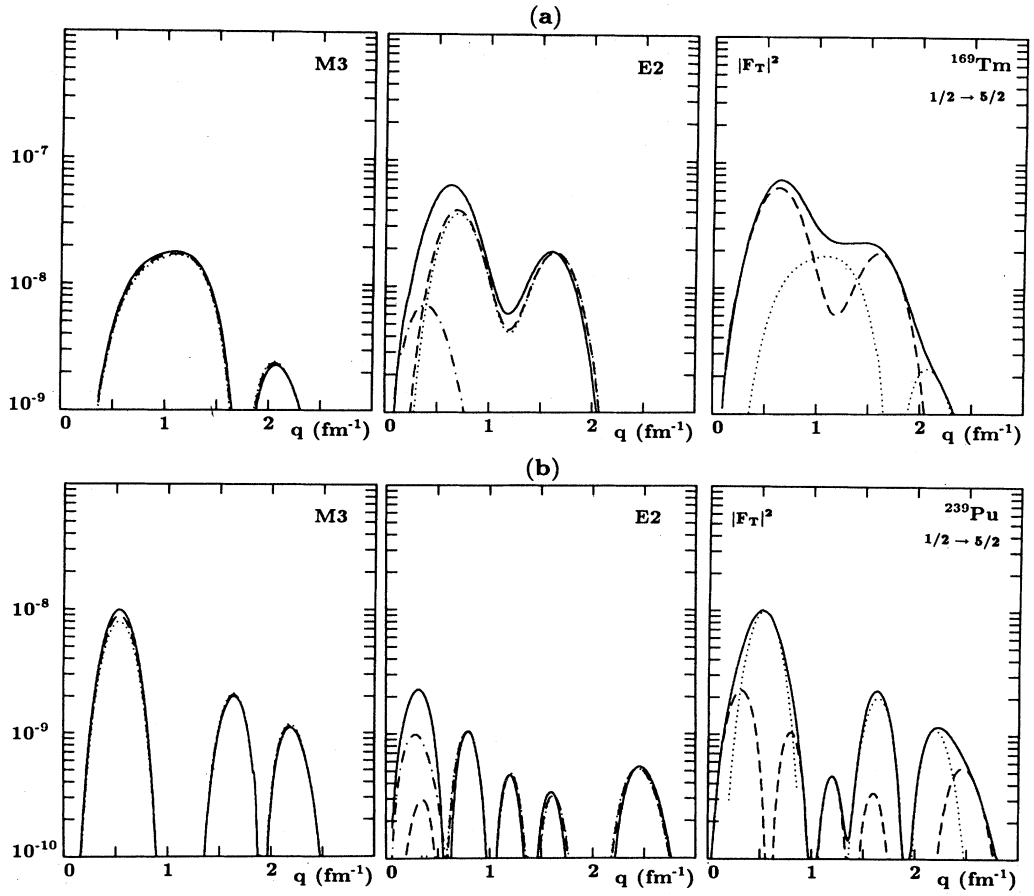

FIG. 4. Same as Fig. 3 for the transition $\frac{1}{2}\rightarrow\frac{5}{2}$ involving the $M3$ and $E2$ multipoles.

add to this a negative amount coming from a negative decoupling parameter and a positive core contribution.[1] Therefore we see an increase in the single-particle form factors when the "a" contribution is added. When the core is taken into account, the contrary effect is found in both nuclei because now a positive core contribution reduces the previous negative single-particle form factor. Also remarkable is the near cancellation of the net core contribution in this case. This is because of the particular values of the Clebsch-Gordan coefficients and of the decoupling parameter that combine to give a negligible addition to the pure single-particle value:

$$-\sqrt{3/5}\mathcal{F}^{E2}_{2k}(\text{s.p.})+\mathcal{F}^{E2}_{R}(a\sqrt{3/5}\sqrt{6}+3\sqrt{2/5}) ,$$

wherein for $a=-0.932$, the factor multiplying the core contribution is 0.129. In the final plots for the total form factors squared, the contributions of the individual multipolarities are shown. The $M1$ dominance in the first peaks is apparent.

For completeness, Figs. 4–5 contain similar results for $\frac{1}{2}\rightarrow\frac{5}{2}$ and $\frac{1}{2}\rightarrow\frac{7}{2}$ transitions, respectively. The same type of analysis applies here for the combinations of all of the various contributions. In both figures the behavior of the electric single-particle multipoles $E2$ and $E4$ are again easily understood from their intrinsic multipoles of Fig. 1. They are simply proportional to the squares of the intrinsic multipoles with coefficients depending on the spin and multipolarity. Nevertheless, the core contributions for the $E2$ multipole in Fig. 4 as compared with the same in Fig. 3 are remarkably important. This is due to the increment in the factor $[I_f(I_f+1)-I_i(I_i+1)]$ for bigger I_f. In ^{239}Pu, the total effect of the $E2$ core contribution is to change the single-particle form factor by more than one order of magnitude. The total form factor for the transition $\frac{1}{2}\rightarrow\frac{5}{2}$ is the sum of the $M3$ and $E2$ multipoles and is also shown in Fig. 4. For the transition $\frac{1}{2}\rightarrow\frac{7}{2}$ in Fig. 5, the collective effects on $M3$ and $E4$ are negligible and the final multipoles are almost completely single-particle. One can also see the different shapes acquired by the $M3$ multipole comparing Fig. 4 and Fig. 5. This is a result of the different spin coefficients with which the single-particle intrinsic multipoles $\mathcal{F}^{M3}_{k,2k}$ are combined to form $F^{M3}_{I_f}$.

V. $k>\frac{1}{2}$ BANDS: ^{177}Hf AND ^{179}Hf

We have selected two odd-neutron nuclei, ^{177}Hf, $k^{\pi}=\frac{7}{2}^{-}$ and ^{179}Hf, $k^{\pi}=\frac{9}{2}^{+}$. The experimental values for the parameters of the rotational model can be extracted in a similar way as in the previous case. The moments of

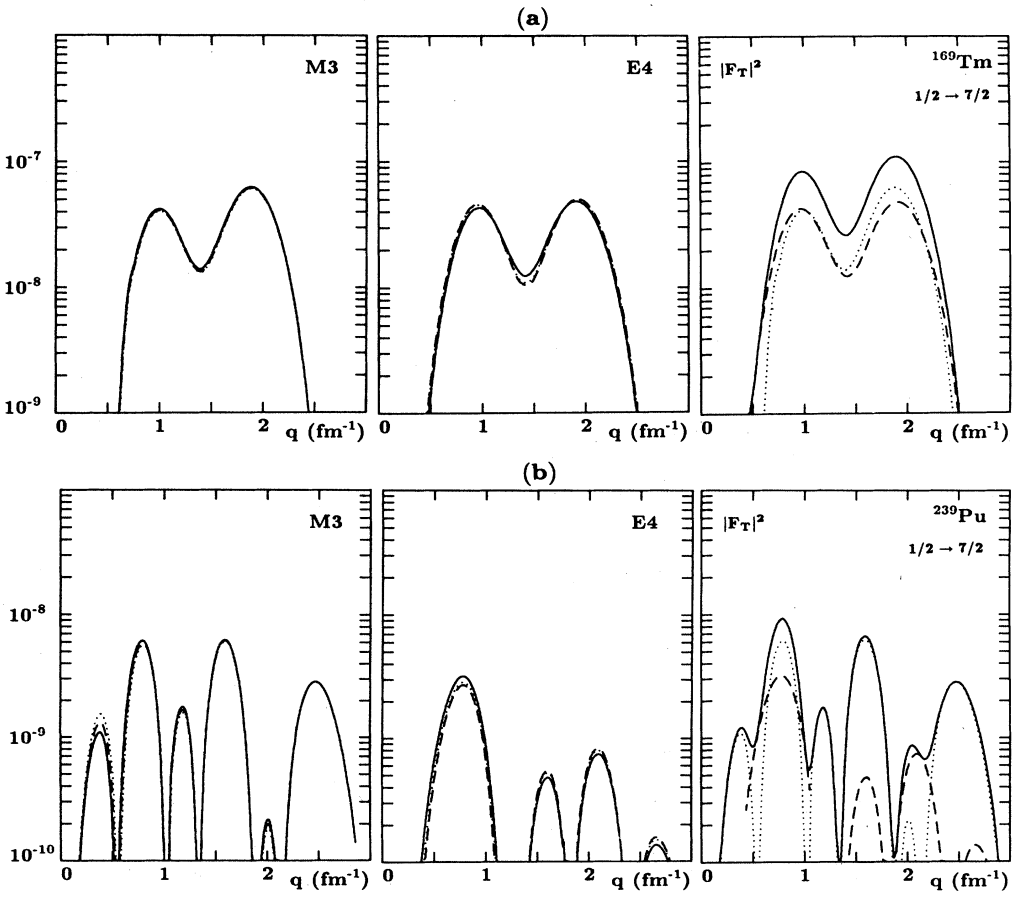

FIG. 5. Same as Fig. 3 for $\frac{1}{2}\rightarrow\frac{7}{2}$ ($M3$ and $E4$ multipoles).

TABLE V. Same as Table IV for the $k > \frac{1}{2}$ nuclei ^{177}Hf and ^{179}Hf.

		g_k	$\mu_{7/2}$	$\mu_{9/2}$	$\mu_{11/2}$	$g_{s_{\text{eff}}}/g_{s_{\text{free}}}$
^{177}Hf	exp	0.216	0.794	1.082	1.48	
	Sk-3	0.447	1.437	1.640	1.867	
			(0.808)	(1.125)	(1.432)	(0.483)
	Ska	0.454	1.444	1.621	1.825	
			(0.797)	(1.091)	(1.377)	(0.476)
	Nilsson	0.373	1.332	1.756	2.174	
			(0.904)	(1.406)	(1.878)	(0.579)
^{179}Hf	exp	−0.207		−0.641		
	Sk-3	−0.373		−1.218	−0.711	
				(−0.608)		(0.555)
	Ska	−0.375		−1.213	−0.679	
				(−0.595)		(0.552)
	Nilsson	−0.344		−0.938	−0.114	
				(−0.433)		(0.601)

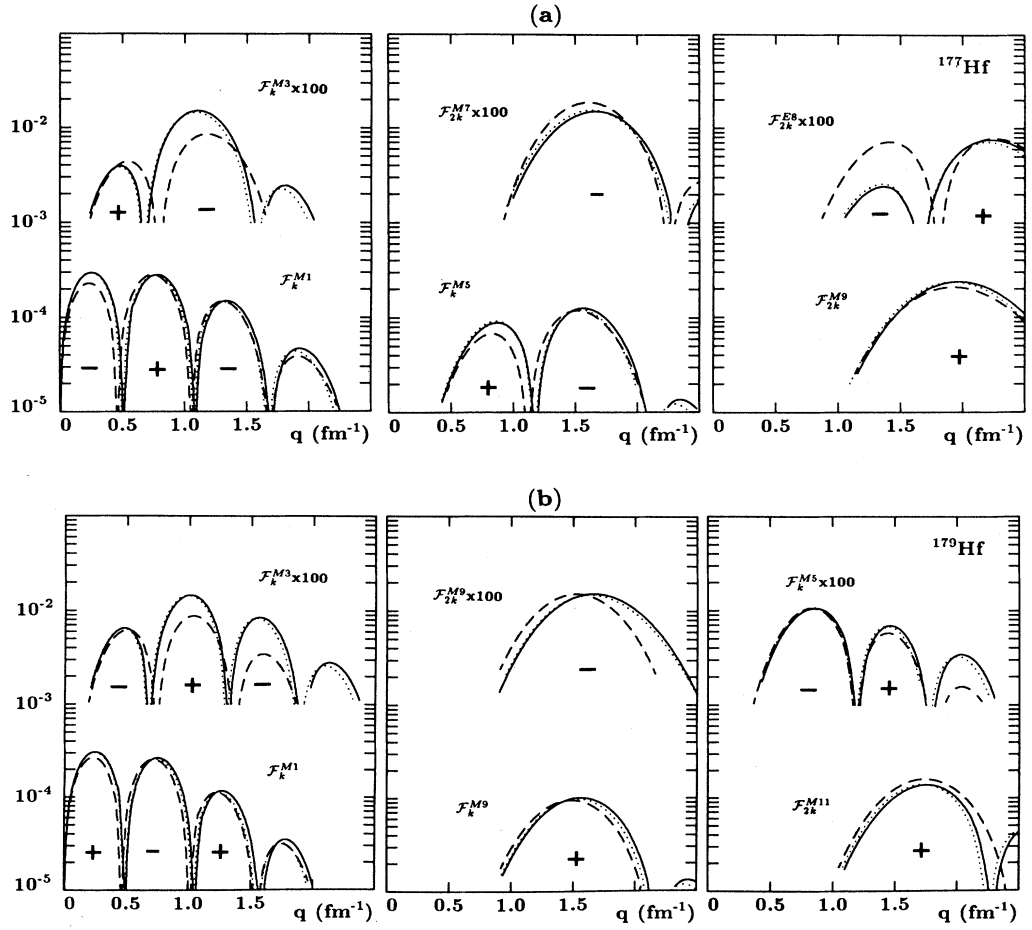

FIG. 6. Intrinsic single-particle form factors of ^{177}Hf (a) and ^{179}Hf (b). Only the most important multipoles are shown. As in Fig. 1, the results are for Sk-3 (solid), Ska (dotted), and Nilsson (dashed).

inertia were inferred from the experimental rotational spectra. In these examples, there is no decoupling parameter and the expression for the energy, Eq. (7), contains only the parameter $\mathcal{J}$, which was obtained from the energy of the first excited state (Table III). From the experimental magnetic moments we can also obtain the parameters g_k and g_R by inverting Eq. (8). Since we have experimental measurements[17] for $\mu_{7/2}$ and $\mu_{9/2}$ for ^{177}Hf, we deduce

$$g_R = -\tfrac{1}{2}\mu_{7/2} + \tfrac{11}{18}\mu_{9/2} ,$$

$$g_k = g_R + \tfrac{99}{98}\mu_{7/2} - \tfrac{77}{98}\mu_{9/2} .$$

These values appear in Tables III and V. They are consistent with the experimental value for $\mu_{11/2}$. They may also be compared with the experimental values $g_k = 0.216(6), g_R = 0.249(8)$ of Ref. 24. In the case of ^{179}Hf, experimental values are available only for the ground state ($\mu_{9/2}$), and then we cannot extract the two parameters needed. For this case we took the values of Ref. 24. Coming back to the calculations, Table III contains the predicted HF moments of inertia and gyromagnetic ratios for these nuclei. The same comments concerning the moment of inertia can be repeated here.

In Table V we compare the experimental g_k and μ_I with Nilsson and HF predictions. One sees again the good agreement obtained when effective g_s factors are used.

For ^{177,179}Hf the Nilsson coefficients, obtained with the parameters shown in Table I, are the following:

^{177}Hf $\frac{7}{2}^-[514]$ $C_{3,7/2} = 0.2873$,

$C_{5,9/2} = 0.9473$,

$C_{5,11/2} = 0.1419$;

^{179}Hf $\frac{9}{2}^+[624]$ $C_{4,9/2} = -0.1273$,

$C_{6,11/2} = -0.0860$,

$C_{6,13/2} = 0.9881$.

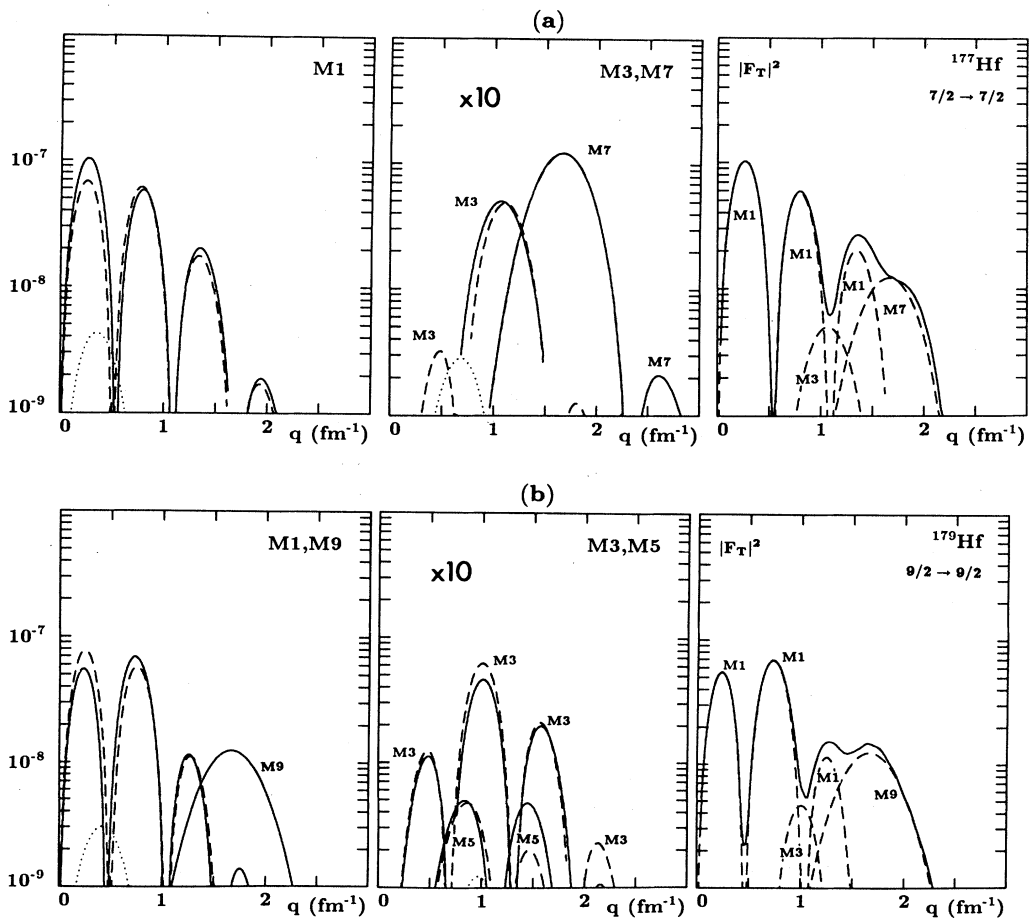

FIG. 7. Total transverse form factor squared of ^{177}Hf (a) and ^{179}Hf (b) in the elastic case ($\frac{7}{2} \to \frac{7}{2}$ and $\frac{9}{2} \to \frac{9}{2}$, respectively). The most important multipolarities for each nucleus are decomposed into their core (dotted) and single-particle (dashed) contributions, to give the total multipolar component of the form factor (solid). In the last panel for each nucleus all the multipolarities, magnetic (dashed) and electric (dotted), are added to give the total transverse form factor (solid).

A. Intrinsic form factors

The single-particle intrinsic form factors can be seen in Fig. 6 for ^{177}Hf (a) and ^{179}Hf (b). Only the most relevant multipoles have been drawn, and again the results correspond to HF calculations with Sk-3 (solid lines) and Ska (dotted) interactions as well as Nilsson (dashed). In order to study the first three transitions for these nuclei, we need the magnetic intrinsic multipoles $M1,3,5,7,9$ and the electric $E2,4,6,8$ for ^{177}Hf. Using them, the transitions $\frac{7}{2}\rightarrow\frac{7}{2}$, $\frac{7}{2}\rightarrow\frac{9}{2}$, and $\frac{7}{2}\rightarrow\frac{11}{2}$ can be constructed. Since in this case $k=\frac{7}{2}$, only $\mathcal{F}^{M\lambda}_{2k}$ with $\lambda=7,9$ are different from zero and for the same reason, intrinsic single-particle electric form factors start only at $E8$. Also, since there is no decoupling parameter, the subscript $2k$ form factors contain no core contribution. Similar comments apply to ^{179}Hf with the difference that now $k=\frac{9}{2}$ and the analysis of multipolarities has to be changed correspondingly. Then, to study the transitions $\frac{9}{2}\rightarrow\frac{9}{2}$, $\frac{9}{2}\rightarrow\frac{11}{2}$, and $\frac{9}{2}\rightarrow\frac{13}{2}$ we need $M1,3,5,7,9,11$ and $E2,4,6,8,10$ and only $M9,11$ and $E10$ contain a $2k$ contribution.

The analysis of the convection and magnetization contributions to the form factors is, in this case, very simple because the magnetization of the odd neutron is dominant by orders of magnitude over its convection term. The similarity in the predictions of the different fields is clear from Fig. 6. For these two nuclei the odd-nucleon wave functions have a much simpler structure than for those considered in Sec. IV. In the Nilsson model one spherical orbital is clearly dominant in each case, carrying 90% of the wave-function normalization. In the Hartree-Fock case the admixtures from $N\neq5$ shells in ^{177}Hf and from $N\neq6$ in ^{179}Hf are less than 10%.

B. Transition form factors

In Figs. 7–9, the elastic case and the transitions to the first and second excited states, respectively, are considered for ^{177}Hf (a) and ^{179}Hf (b).

Results are for the Sk-3 force with the cranking model, and in each figure, the first two drawings are the decomposition of the multipoles into the core (dotted) and single-particle (dashed) contributions to give the total $|\mathcal{F}^{\sigma\lambda}_{I_f}|^2$ as solid lines, while the third plot corresponds to the sum of all of the multipolarities (dashed for magnetic and dotted for electric) to give the total transverse form factor of Eq. (1).

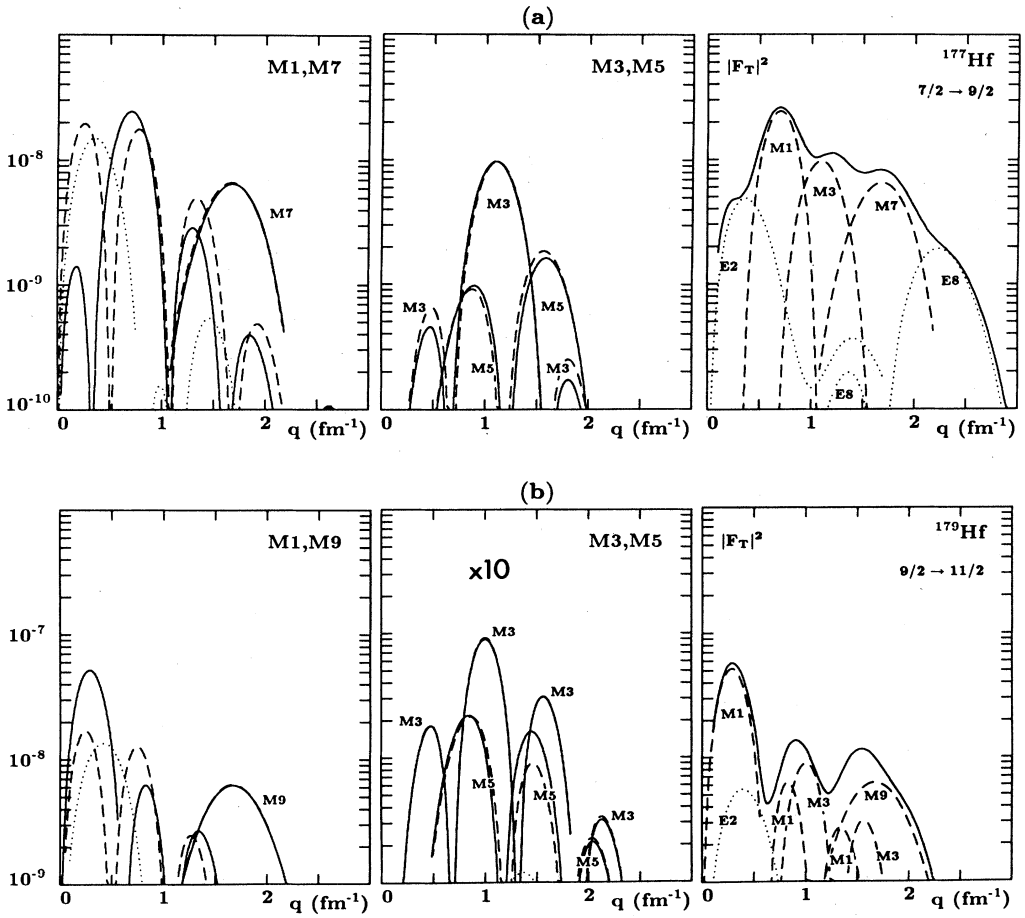

FIG. 8. Same as Fig. 7 for the transition $\frac{7}{2}\rightarrow\frac{9}{2}$ and $\frac{9}{2}\rightarrow\frac{11}{2}$ in ^{177}Hf and ^{179}Hf, respectively.

The analysis is much simpler than in the $k=\frac{1}{2}$ cases discussed in Sec. IV. The single-particle contribution is simply proportional to the square of the intrinsic form factor for the multipolarities $M1,M3,M5$ in ^{177}Hf and $M1,M3,M5,M7$ in ^{179}Hf. For the higher multipolarities it is a linear combination of the subscript k and $2k$ parts. In Fig. 7 the elastic case is considered and then only magnetic multipoles contribute. For ^{177}Hf $M5$ is negligible in the whole range of q. For $M1$ and $M3$ the result of combining the single particle with the core has opposite effects in the first peak: While they add in $M1$, they subtract in $M3$. The total form factor is almost entirely $M1$ up to $q=1.5$ fm^{-1} and dominated by $M7$ afterwards. In ^{179}Hf, the situation is very similar with a dominant $M1$ at low q and in this case $M9$ at high q.

The reduction of the multipoles as compared to the spherical case is a well-known characteristic of the deformed model.[2] This reduction can well be analyzed in terms of the Nilsson model, for which expressions for the quenching factors can be explicitly written.[25] Especially important is the suppression of the $M5$ multipole in ^{177}Hf as well as $M7$ in ^{179}Hf. This is due to the Clebsch-Gordan coefficient of Eq. (2) for these multipolarities. In particular, for ^{177}Hf one can obtain, from the corresponding values of the Clebsch-Gordan coefficients squared, reduction factors of 0.016 for the intrinsic $M5$ multipole but only of 0.212 for $M3$ and 0.818 for $M1$.

In general, for both nuclei, the core contribution is responsible for a change of the first peak by a factor 1.5 relative to the single particle, but in opposite directions. The single-particle and collective contributions add constructively in ^{177}Hf and destructively in ^{179}Hf. The reason for this different behavior in the two nuclei is the opposite sign of their single-particle form factors (Fig. 6).

In Fig. 8, transitions to the first excited state are considered. The most remarkable feature is the strong suppression of the $M1$ first peak in ^{177}Hf and the opposite situation for ^{179}Hf. In ^{177}Hf the core almost cancels the single-particle contribution (reducing the peak by a factor 10), while in ^{179}Hf it produces an enhancement of a factor 2.5. The reason for this is that now the spin-dependent coefficient of the core term is large, and this makes it comparable to the single-particle term. This coefficient has a different sign than in the elastic case where the core acts in the opposite direction. One can see from the total form factor the importance of the core contribution in this case. In ^{177}Hf, due to the cancellation in the $M1$ multipole at low q, the form factor is almost solely the core $E2$ contribution, up to $q=0.4$ fm^{-1}. On the other hand, ^{179}Hf has a big peak formed by $M1$ and to a lesser

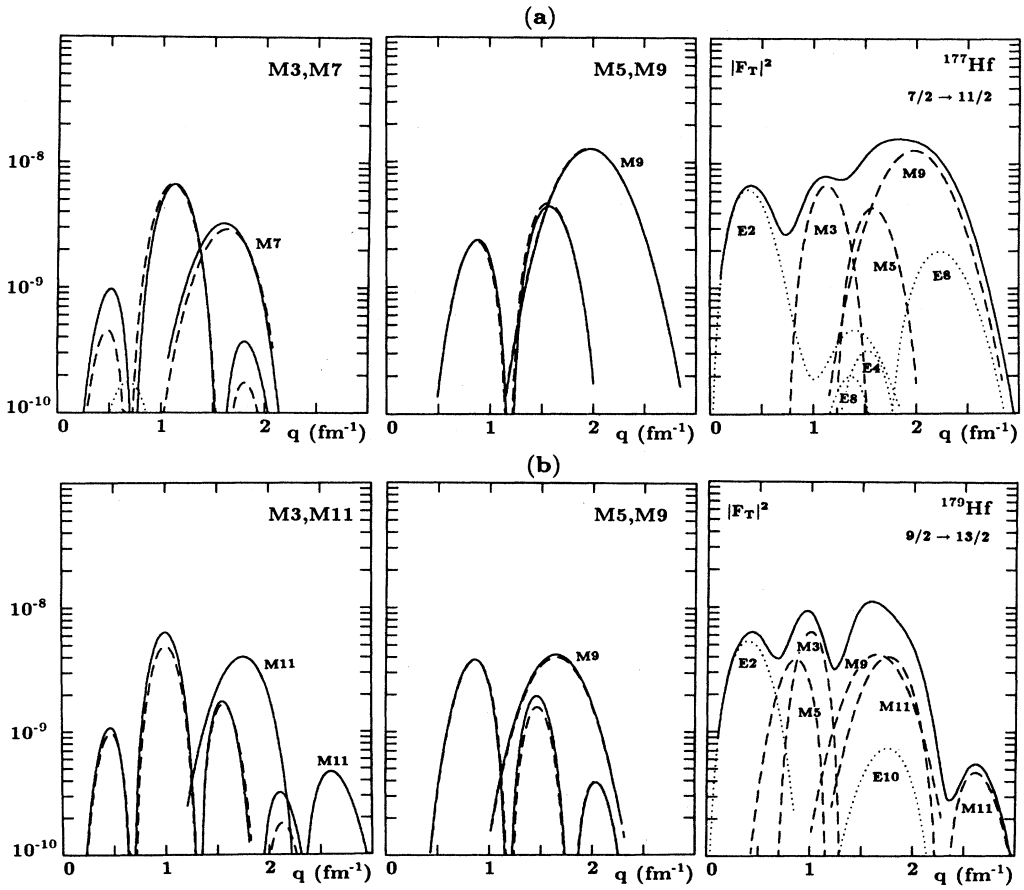

FIG. 9. Same as Fig. 7 for $\frac{7}{2}\rightarrow\frac{11}{2}$ in ^{177}Hf and $\frac{9}{2}\rightarrow\frac{13}{2}$ in ^{179}Hf.

extent by the collective $E2$. In the figures for the total form factor, only the main peaks have been plotted.

Finally, in Fig. 9, we can see the form factors for the transition to the second excited state. In this case no $M1$ contribution exists and then the total form factor is purely the $E2$ collective contribution in the low q range $0 < q < 0.7$ fm^{-1} in both nuclei. This produces a total form factor at low q quite similar for the two isotopes. However, at higher q the total form factors exhibit quite different structure for ^{177}Hf and for ^{179}Hf. This is due to the different multipolarities and single-particle wave functions that enter in each case.

VI. CONCLUSIONS AND FINAL REMARKS

We have presented a detailed analysis of the transverse form factors for several representative odd-A nuclei for elastic and inelastic electron scattering within the ground-state rotational band. The form factors have been decomposed into their collective and single-particle contributions for each multipolarity, stressing their relative importance in the different q ranges with special attention to the $k = \frac{1}{2}$ nuclei for which the core contribution is particularly involved. We have also studied the mean field dependence of the single-particle form factors by comparing the predictions of HF+BCS with two different effective interactions as well as with the Nilsson model.

From the results obtained, we can conclude that the single-particle form factors are not very sensitive to the mean field used in the generation of the wave functions. In particular Sk-3 and Ska predict almost the same result. Even the Nilsson model, in most instances, produces a structure similar to that of the Skyrme interactions.

Concerning core and single-particle interplay, we can say as a general result that the core manifests itself only in the low-q region ($q < 1$ fm^{-1}) where it interferes with the single-particle contribution. In this region the interference can be constructive or destructive depending on the nucleus and on the specific transition, leading in some cases to very large effects. For larger q, the dominant role is played by the single-particle aspect and the form factors reflect the properties of the odd nucleon, in contrast to what happens in longitudinal form factors[26] where all the nucleons contribute to the charge density.

Combining these results with the rotational model dependence analysis of Ref. 1 and for the lower multipoles $M1$ and $E2$ (for which the single-particle and core interference is most significant) we can conclude that since the rotational $M1$ multipole is not very sensitive to the model employed to describe the band, we expect for this multipole the same results even for the macroscopic models. On the other hand, the collective $E2$ is strongly model dependent and we expect important changes in the $q < 1$ fm^{-1} region for this multipole if a different rotational model is used.

A comparison of the form factors for these nuclei shows the rich variety of shapes expected for the transverse form factors of odd-A rotators. Besides the core influence at low q, the changes are mainly due to the different k values for the ground-state rotational band which dictate the strength of the Clebsch-Gordan coefficients.

At the present time the only extensive set of data for an odd-Z rotational nucleus is for ^{181}Ta.[27] We believe it would be interesting to study other odd-A rotational nuclei, particularly $k = \frac{1}{2}$ cases such as those discussed in this paper. Such data would allow a searching test of the applicability of the rotational model.

ACKNOWLEDGMENTS

This work was supported in part by operating Grant A-3198 of the Natural Sciences and Engineering Research Council of Canada (D.W.L.S. and P.S.); and by Contract PB87/0311 of the Dirección General de Investigación Científica y Técnica [DGICYT (Spain)] (E.M.G. and P.S.). E.M.G. also acknowledges support of a collaborative research Grant 0702/87 from NATO, and expresses her thanks to the McMaster Physics Department for their kind hospitality. P.S. is grateful to the Consejo Superior de Investigaciones Científicas for a postdoctoral fellowship.

[1] D. Berdichevsky, P. Sarriguren, E. Moya de Guerra, M. Nishimura, and D. W. L. Sprung, Phys. Rev. C **38**, 338 (1988).
[2] E. Moya de Guerra, Phys. Rep. **138**, 293 (1986).
[3] E. Moya de Guerra, Ann. Phys. (N.Y.) **128**, 286 (1980).
[4] E. Moya de Guerra and S. Kowalski, Phys. Rev. C **22**, 1308 (1980); **20**, 357 (1979).
[5] F. Beiner, H. Flocard, N. Van Giai, and P. Quentin, Nucl. Phys. **A238**, 29 (1975).
[6] H. S. Köhler, Nucl. Phys. **A258**, 301 (1976).
[7] T. de Forest and J. D. Walecka, Adv. Phys. **15**, 1 (1966).
[8] D. Vautherin, Phys. Rev. C **7**, 296 (1973).
[9] D. W. L. Sprung, S. G. Lie, M. Vallières, and P. Quentin, Nucl. Phys. **A326**, 37 (1979); D. W. L. Sprung, S. G. Lie, and M. Vallières, Nucl. Phys. **A352**, 19 (1981).
[10] G. G. Simon, Ch. Schmitt, F. Borkowski, and V. H. Walther, Nucl. Phys. **A333**, 381 (1980).
[11] H. Chandra and G. Sauer, Phys. Rev. C **13**, 245 (1976).
[12] S. G. Nilsson, C. F. Tsang, A. Sobiczewski, Z. Szymanski, S. Wycech, C. Gustafson, I.-L. Lamm, P. Möller, and B. Nilsson, Nucl. Phys. **A131**, 1 (1969).
[13] I.-L. Lamm, Nucl. Phys. **A125**, 504 (1969).
[14] J. Rekstad and G. Løvhøiden, Nucl. Phys. **A267**, 40 (1976).
[15] K. E. G. Löbner, M. Vetter, and V. Hönig, Nucl. Data Tables **A7**, 495 (1970).
[16] H. Flocard, P. Quentin, A. K. Kerman, and D. Vautherin, Nucl. Phys. **A203**, 433 (1973).
[17] P. Raghavan, report, Rutgers University, 1988 (submitted to At. Data Nucl. Data Tables).
[18] C. M. Lederer and V. S. Shirley, *Table of Isotopes* (Wiley, New York, 1978).
[19] J. D. Bowman, J. de Boer, and F. Boehm, Nucl. Phys. **61**, 682

(1965).
[20]F. Boehm, G. Goldring, G. B. Hagermann, G. D. Symons and A. Tveter, Phys. Lett. **22**, 627 (1966).
[21]K. Hardt, P. Schüler, C. Günther, J. Recht, and K. P. Blume, Z. Phys. A **314**, 83 (1983).
[22]A. Arima, K. Shimizu, W. Bentz, and H. Hyuga, Adv. Nucl. Phys. **18**, 1 (1988).
[23]A. Bohr and B. Mottelson, *Nuclear Structure* (Benjamin, New York, 1975), Vol. II.
[24]S. Büttgenbach, M. Herschel, G. Meisel, E. Schrödl, and W. Witte, Phys. Lett. **43B**, 479 (1973); Z. Phys. **260**, 157 (1973).
[25]E. Graca, P. Sarriguren, D. Berdichevsky, D. W. L. Sprung, E. Moya de Guerra, and M. Nishimura, Nucl. Phys. **A483**, 77 (1988).
[26]W. Bertozzi, Nucl. Phys. **A374**, 109c (1982).
[27]F. N. Rad, W. Bertozzi, S. Kowalski, C. P. Sargent, C. F. Williamson, M. V. Hynes, B. Norum, B. Peterson, T. Sasanuma, and W. Turchinetz, Phys. Rev. Lett. **45**, 1758 (1980).